

5,5'-二甲基乙内酰脲体系电沉积金

杨潇薇^{1,2} 张云望¹ 安茂忠² 张 林^{*,1}

(¹ 中国工程物理研究院激光聚变研究中心, 绵阳 621900)

(² 哈尔滨工业大学化工学院, 哈尔滨 150001)

摘要: 开发了以 5, 5'-二甲基乙内酰脲(DMH)为配位剂的无氰电镀金工艺。利用扫描电镜(SEM)和线性扫描伏安曲线对电镀时间和添加剂(由丁炔二醇、糖精和十二烷基硫酸钠组成)对镀金层表面、断面形貌和镀液性能的影响进行了测试,结果表明随着电镀时间的延长镀金层表面形貌几乎没有发生变化,光亮剂的加入增大了阴极极化同时使镀金层结晶变得细致均匀,在由 H₂AuCl₄, DMH, K₃PO₄ 和 KH₂PO₄ 组成的基础镀液中金的沉积速度可达 0.3 $\mu\text{m} \cdot \text{min}^{-1}$,镀液中添加剂的加入没有影响金的沉积速度。利用 X 射线衍射技术(XRD)和 X 射线光电子能谱技术(XPS)对镀金层性能进行了测试,结果表明镀金层沿着(111)晶面择优生长并且由纯金组成。利用循环伏安曲线和旋转圆盘电极对 Au(III)在镀液中的电化学还原机制进行了研究,结果表明当研究电极为玻碳电极(GCE),镀液温度为 45 $^{\circ}\text{C}$ 时,镀液中金的电沉积过程是受扩散控制的不可逆的过程。同时利用循环伏安曲线对镀金液的稳定性进行了分析。

关键词: 电沉积金; 无氰; 5, 5'-二甲基乙内酰脲; 循环伏安; 旋转圆盘电极

中图分类号: TQ153.1

文献标识码: A

文章编号: 1001-4861(2012)12-2617-09

Electrodeposition of Gold from Non-cyanide Bath Using 5, 5'-Dimethylhydantoin-gold Complex

YANG Xiao-Wei^{1,2} ZHANG Yun-Wang¹ AN Mao-Zhong² ZHANG Lin^{*,1}

(¹Research Center of Laser Fusion, China Academy of Engineering Physics, Mianyang, Sichuan, 621900, China)

(²School of Chemical Engineering and Technology, Harbin Institute of Technology, Harbin 150001, China)

Abstract: The effect of plating time and brightening additives (composed of saccharin, butynediol and sodium dodecyl sulfate) on the properties of gold deposits plated from a non-cyanide bath with 5, 5'-dimethylhydantoin (DMH) as the complexing agent was investigated by using scanning electron microscopy (SEM) and linear sweep voltammetry measurements. The results indicate that surface morphologies of gold electrodeposits are not markedly affected and do not change significantly with increasing deposition time, and brightening additives increase the cathodic polarization of bath and refine the grains of electrodeposits. The gold deposition rate in basic bath containing H₂AuCl₄, DMH, K₃PO₄, KH₂PO₄ is 0.3 $\mu\text{m} \cdot \text{min}^{-1}$, and the high deposition rate is not influenced by the introduction of brightening additives. The properties of electrodeposits were evaluated by X-ray diffraction (XRD) and X-ray photoelectron spectroscopy (XPS). The results show that the gold electrodeposits have a preferential orientation along (111) direction and are composed of pure Au⁰ state. The electrochemical behavior of Au(III) in the bath onto glassy carbon electrode (GCE) at 45 $^{\circ}\text{C}$ was studied by cyclic voltammetry and standard rotating disk. The results indicate that the electrodeposition of metallic Au in the bath is an irreversible process and is controlled by the diffusion of Au (III) onto GCE. The stability of the DMH-gold bath is also discussed.

Key words: gold electrodeposition; non-cyanide; 5, 5'-dimethylhydantoin; cyclic voltammograms; rotating disc electrode

收稿日期: 2012-03-16。收修改稿日期: 2012-06-19。

中国工程物理研究院激光聚变研究中心资助项目。

*通讯联系人。E-mail: address: zhlmy@sina.com

The combination of excellent electrical conductivity, solderability and bondability with high corrosion resistance has led to the widespread adoption of gold as a standard material for numerous applications in microelectronic, optoelectronic and microsystem technologies^[1-4]. However, due to the high intrinsic cost of gold, it is important and advantageous to identify the type of plating baths which can offer the best gold deposits for a deposition process.

For many decades, cyanide-containing baths for gold electrodeposition have been used. On the one hand, the gold (I) cyanide complex has a stability constant of 10^{39} , which makes the solution very stable, and cyanide salts are also very cheap. On the other hand, cyanide is very poisonous even at a very low concentration, which can lead to difficulties in plating operation and waste disposal^[5-6]. Therefore, the demand for non-cyanide gold electroplating processes has increased significantly. A number of attempts to produce gold electrolytes from iodide, hydroxide, thiosulfate, sulfite and phosphoric acid were made^[7-9]. Of these, sulfite is the most commonly used complex for gold deposition as an alternative to the cyanide electrolyte and has been widely studied and utilized. It can produce fine, smooth and bright gold deposits and is non-toxic and suitable for plating soft gold in the micro-electronics industry. However, the disadvantage of sulfite electrolyte is instability. To counteract this stability problem, many Au (I) sulfite baths are operated at $\text{pH} \geq 8$ or have been added various additives (such as 2, 2'-dipyridine, ethylenediamine or aromatic nitro-compounds)^[10-12]. More recently, a non-cyanide bath containing both thiosulfate and sulfite as complexing agents was reported. It was found that mixed sulfite bath had higher stability than either the pure sulfite or thiosulfate bath, and did not require the use of stabilizers. However, the preparation procedure was very complicated, not only in terms of controlling the pH value, but also in terms of the mixing sequence^[13]. In addition to sulphite and sulphite-thiosulphate baths, gold plating bath employing 5, 5'-dimethylhydantoin (DMH) was also been proposed^[14].

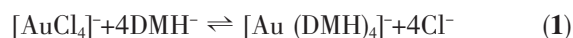
The DMH is nontoxic and can form stable complex with Au (III). The addition of thallium ions, as a grain refiner have been found to reduce the grain size and increase the brightness of deposits. Under optimum plating conditions the deposits are smooth, uniform and dense. However, there is a serious problem with this electrolyte. Toxicity of thallium (human poison; lethal dose approximately $0.1 \text{ mg} \cdot \text{m}^{-3}$) is of concern. In a subsequent study, our group developed a similar electrolyte using DMH as complexing agent. However, thallium was not used as grain refiner by the previous researchers. This novel electrolyte is highly stable, non-toxic and also can produce thick gold electrodeposits. The high plating rate which has been little published is very important in some industrial fields of gold plating. The aim of our present work is to develop bright gold deposits with the thickness of $(18 \pm 2) \mu\text{m}$, while the deposits plated from this novel electrolyte can satisfy the specific thickness demand of gold plating applications.

This paper reports a new hydantoin based pure gold electroplating process with excellent stability. The effects of the plating time and composition of gold plating bath using various brightening additives on deposition are investigated. The process characterization, including deposit morphology, thickness, composition and solution stability is presented. The electrochemical behavior is evaluated by cyclic voltammetry and polarisation measurements.

1 Experimental

1.1 Gold electroplating

The basic bath was prepared by dissolving $0.625 \text{ mol} \cdot \text{L}^{-1}$ of DMH in deionised water. Once dissolved, the pH value of the solution was adjusted to 9~10 with the addition of KOH, followed by the addition of $0.05 \text{ mol} \cdot \text{L}^{-1}$ of HAuCl_4 . The $[\text{AuCl}_4]^-$ subsequently underwent a homogeneous reduction reaction to form a DMH-gold ligand in solution:



This solution was light yellow initially, within a few hours under stirring it became transparent until the HAuCl_4 was fully complexed with DMH. The

solution stayed transparent with a faint yellowish color for the whole testing period. Then, $0.4 \text{ mol} \cdot \text{L}^{-1}$ of K_3PO_4 was added to the solution and the pH value of the final electrolyte was adjusted to 9~10 by the addition of KH_2PO_4 . Besides the basic bath, other electroplating baths were prepared by adding brightening additives (composed of saccharin, butynediol and sodium dodecyl sulfate).

The composition and operating conditions of the

gold electrodeposition bath used in this study were listed in Table 1. The substrates used were copper sheets ($10 \text{ mm} \times 10 \text{ mm} \times 0.1 \text{ mm}$) pretreated by immersion in a solution of 50% hydrochloric acid, and rinsed with distilled water. Copper, as cathode material, was used because it was isostructural with gold with a nearly identical lattice content, which avoided surface from cracks and minimized microstrain in the deposit.

Table 1 Compositions and conditions of plating bath using the DMH-gold complex

$c_{\text{HAuCl}_4} / (\text{mol} \cdot \text{L}^{-1})$	0.05
$c_{\text{DMH}} / (\text{mol} \cdot \text{L}^{-1})$	0.625
$c_{\text{K}_3\text{PO}_4} / (\text{mol} \cdot \text{L}^{-1})$	0.4
$c_{\text{KH}_2\text{PO}_4} / (\text{mol} \cdot \text{L}^{-1})$	calculated
Brightening additives (composed of saccharin, butynediol and sodium dodecyl sulfate)	—
pH value	9~10
Temperature / $^{\circ}\text{C}$	45
Current density / ($\text{A} \cdot \text{dm}^{-2}$)	1.5
Plating time / min	10~60
Stir	mild

1.2 Electrochemical evaluation

Cyclic and linear sweep voltammetry measurements were carried out in a three-electrode glass cell on a GAMRY Reference 600 electrochemical workstation. A glassy carbon electrode (GCE) and a rotating disk electrode (RDE) with a working surface of 0.07 cm^2 ($\varphi=0.3 \text{ cm}$) were used as the working electrode (WE), the RDE was also a GCE embedded in teflon in conjunction with a speed control unit, the counter electrode (CE) was a platinum plate and the reference electrode was a saturated calomel electrode (SCE). The bath temperature was maintained at $45 \text{ }^{\circ}\text{C}$ by thermostat control. The cathodic polarisation curves were recorded at a scanning rate of $1 \text{ mV} \cdot \text{s}^{-1}$, and rotation speed of the RDE ranged from 50 to $400 \text{ rad} \cdot \text{s}^{-1}$. Cyclic voltammetry sweeps were recorded as a function of scan rate from 10 to $90 \text{ mV} \cdot \text{s}^{-1}$.

1.3 Characterizations of gold electrodeposits

The surface and cross-sectional morphologies of the samples were measured by field emission scanning

electron microscopy (FE-SEM, Hitachi S4700) at 25 kV working voltage. The X-ray diffraction (XRD) analysis was carried out with a scanning rate of $0.02^{\circ} \cdot \text{s}^{-1}$ with Cu $K\alpha$ radiation ($\lambda=0.154 \text{ nm}$). The chemical composition of the deposits was probed using Physical Electronics, PHI 5700 EICA X-ray photoelectron spectroscopy (XPS) with Al $K\alpha$ (1486.6 eV) monochromatic source. Data was taken after 120 s of ion etching. All energy values were corrected using C1s at 284.62 eV as a reference.

2 Results and discussion

2.1 Effect of plating time on microstructures of electrodeposits

Because the main aim of developing this bath is to apply it to some thick gold plating fields, the deposition rate is desired to be as high as possible. Our investigation reveals that the plating rate in the bath without or with brightening additives both can reach about $0.3 \text{ } \mu\text{m} \cdot \text{min}^{-1}$, which is very effective for achieving our purpose. After electrodeposition, the

copper substrates are covered by gold film with a golden-brown or bright golden-brown color. And it also can be noted that all samples have been completely covered with films and are uniform in appearance. To investigate the influences of plating time, the SEM plan views of gold deposits plated from the bath without or with brightening additives at $1.5 \text{ A} \cdot \text{dm}^{-2}$ for different plating time were studied.

For a constant deposition time of 10 min (Fig.1a), the films are continuous and adherent to the substrate. They consist of large gold particles about $0 \sim 0.5 \mu\text{m}$ average diameter, frequently aggregate in clusters with typical sizes in the range of $0.5 \sim 1 \mu\text{m}$. Increasing the deposition time to 40 ~60 min (Fig.1b and c) the number and size of gold particles are not changed significantly and the morphology of the film is not modified, indicating that the properties of DMH-gold plating bath is very stable. Overall, from Fig.1a, b and

c, on can see that the deposits plated in basic bath consist of dense and relatively smooth homogeneous particles, and the morphology and particle size are only varied slightly with the deposition time. The surface morphologies of deposits are shown in Fig.1d, e and f. By applying different deposition time, *i.e.* 10, 40 and 60 min, it also can be seen that the number and size of gold particles are changed significantly with the extension of deposition time. The only difference is that the gold grains become smaller compared with that of deposits plated in basic bath and the gold film is bright golden-brown in color. So, it can be concluded that from Fig.1 the morphologies of gold deposits plated in bath without or with brightening additives are varied slightly with the deposition time. The properties of DMH-gold plating bath and the technology process are very stable and viable for plating for long time.

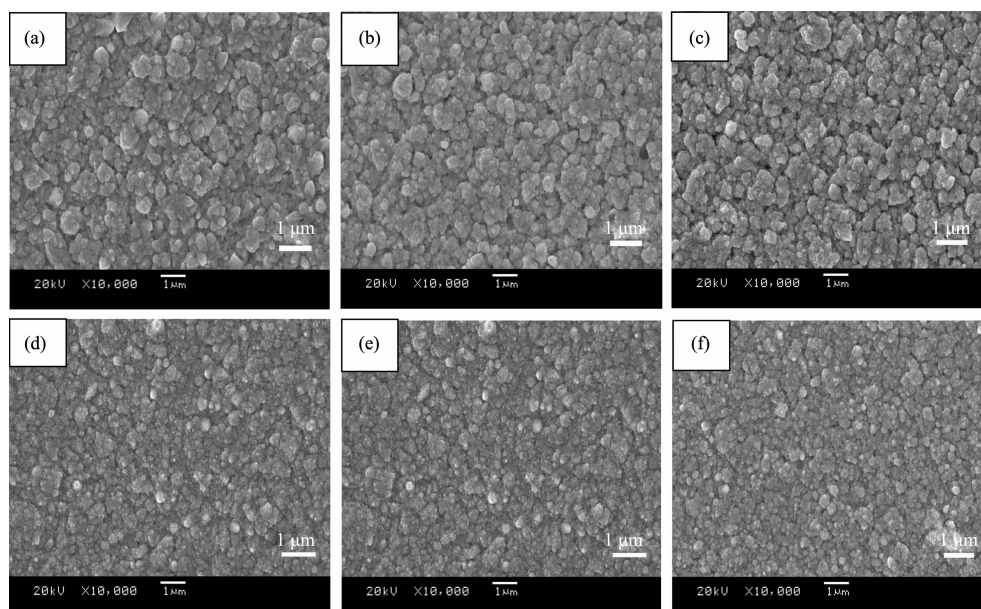


Fig.1 Surface morphologies of gold electrodeposits plated at $1.5 \text{ A} \cdot \text{dm}^{-2}$ for (a) 10 min; (b) 40 min; (c) 60 min in bath without additives and (d) 10 min; (e) 40 min; (f) 60 min in bath with brightening additives

The effect of deposition time on the cross-sectional morphologies of gold deposits formed in DMH-gold bath without or with brightening additives can be ascertained by comparing the films depicted in Fig.2.

The SEM images of deposits display a compact film, with almost no defects in the deposited regions.

In the SEM images of gold deposits shown in Fig.2a and c synthesized by 40-min depositions, the consecutive depositions of gold reach thickness of 12.10 and $10.57 \mu\text{m}$, respectively. The thickness of the deposits increase with increasing deposition time, and the deposit thickness is increased to 21.47 and $20.20 \mu\text{m}$ when samples are electrodeposited for 60

min shown in Fig.2b and d, respectively. It also noted that the average thickness calculated from the weight gain of gold deposits is in agreement with the thickness shown in the micrograph (Fig.2). Therefore, these results suggest that the gold average deposition rates in both baths are similar (about $0.3 \mu\text{m} \cdot \text{min}^{-1}$), which can achieve the purpose of electroplating thick gold deposit. The maximum thickness of gold deposits

with uniform appearance plated in DMH-gold bath can reach about $24 \mu\text{m}$, and the samples are plated about 80 min at $1.5 \text{ A} \cdot \text{dm}^{-2}$. If the plating time is prolonged, the uniformity and color of the gold deposits will become worse. So the controllable range of deposition thickness plated in the DMH-gold bath in this work is $0 \sim 24 \mu\text{m}$.

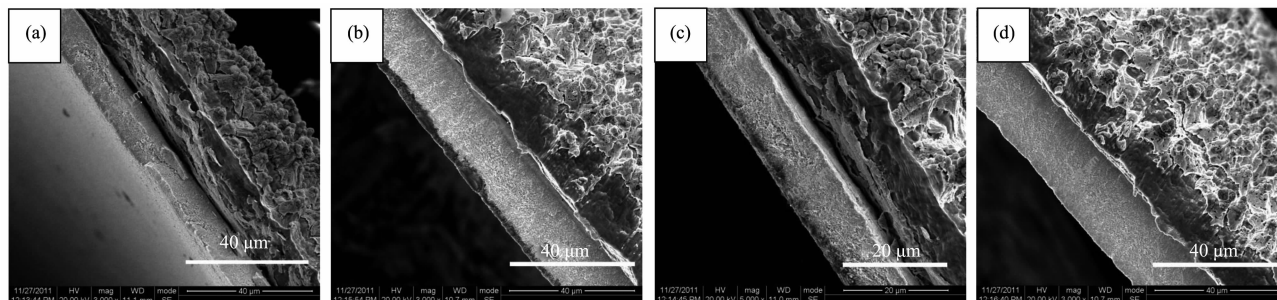


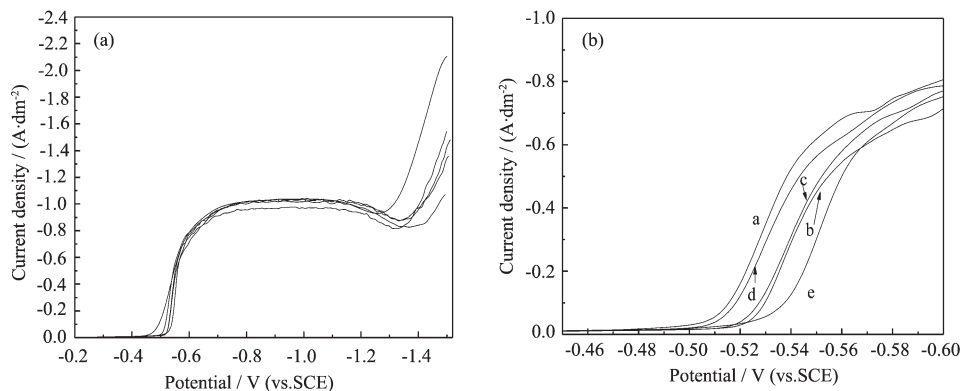
Fig.2 Cross-sectional morphologies of gold deposits plated at $1.5 \text{ A} \cdot \text{dm}^{-2}$ for (a) 40 min; (b) 60 min in bath without additives and (c) 40 min; (d) 60 min in bath with brightening additives

2.2 Effect of the addition of brightening additives in the basic bath

Before discussing the effect of additives on deposit morphology, it will be useful to present their effect on the electrode response during Au (III) reduction.

Fig.3 shows polarization curves for gold deposition obtained in the absence of additives (a) and in the presence of brightening additive (b~e). Fig.3b is the magnified result of Fig.3a for the scanning potential range from -0.45 V to -0.60 V .

Comparison of curves (a) and (b)~(e) shown in Fig.3b indicates that the curves obtained in the solutions containing additives are polarized toward more negative potential relative to that of an additive-free bath. The cathodic potential of -0.55 V is the lowest for curve (e). The results shown in Fig.3 suggest that the adsorption of brightening additives at the electrode surface would be expected to inhibit gold reduction. In general, a higher cathodic polarization accelerates the growth of finer grains. Then, preliminary gold deposition studies show that



(a) basic bath; (b) basic bath+ $1.2 \text{ mmol} \cdot \text{L}^{-1}$ of butynediol; (c) basic bath+ $0.55 \text{ mmol} \cdot \text{L}^{-1}$ of saccharin; (d) basic bath + $0.17 \text{ mmol} \cdot \text{L}^{-1}$ of sodium dodecyl sulfate; (e) basic bath+ $1.2 \text{ mmol} \cdot \text{L}^{-1}$ of butynediol+ $0.55 \text{ mmol} \cdot \text{L}^{-1}$ of saccharin+ $0.17 \text{ mmol} \cdot \text{L}^{-1}$ of sodium dodecyl sulfate.

Fig.3 LSV curves of various baths at the scanning rate of $1 \text{ mV} \cdot \text{s}^{-1}$

the addition of brightening additives to the basic bath leads to brighter gold deposits. And the optimum composition of brightening additive in the DMH-gold bath is $0.55 \text{ mmol} \cdot \text{L}^{-1}$ of saccharin, $1.2 \text{ mmol} \cdot \text{L}^{-1}$ of butynediol and $0.17 \text{ mmol} \cdot \text{L}^{-1}$ of sodium dodecyl sulfate.

Fig.4. SEM images of gold electrodeposited from various baths at $1.5 \text{ A} \cdot \text{dm}^{-2}$ for 10 min on copper sheets: (a) basic bath; (b) basic bath+ $1.2 \text{ mmol} \cdot \text{L}^{-1}$ of butynediol; (c) basic bath + $0.55 \text{ mmol} \cdot \text{L}^{-1}$ of saccharin; (d) basic bath+ $0.17 \text{ mmol} \cdot \text{L}^{-1}$ of sodium dodecyl sulfate; (e) basic bath + $1.2 \text{ mmol} \cdot \text{L}^{-1}$ of butynediol+ $0.55 \text{ mmol} \cdot \text{L}^{-1}$ of saccharin+ $0.17 \text{ mmol} \cdot \text{L}^{-1}$ of sodium dodecyl sulfate.

The deposit shown in Fig.4a clearly shows a rough surface because of the absence of additives in basic bath. Deposit (a) is golden-brown in color and has obvious gold grains in larger size. In fact, it is impossible to produce commercially acceptable deposits from a simple DMH-gold electrolyte without any additives. In Fig.4b and c, the number and size of large gold particles decrease and agglomeration of grains is found for the gold deposits plated from bath b and bath

c(containing $1.2 \text{ mmol} \cdot \text{L}^{-1}$ of butynediol or $0.55 \text{ mmol} \cdot \text{L}^{-1}$ of saccharin). This phenomenon is attributable to the absorption of butynediol or saccharin at the cathode and the grains of deposit b and deposit c are finer than that of deposit a. The result is consistent with the results in Fig.3. In order to gain much smaller grains and smoother micro-surface, $0.17 \text{ mmol} \cdot \text{L}^{-1}$ of sodium dodecyl sulfate was added into bath a and the corresponding SEM morphologies is shown in Fig.4d. From a comparison of Fig.4d and a, the addition of sodium dodecyl sulfate in bath a does not show significant influences on the resultant morphology. As shown in Fig.4e, after the addition of sodium dodecyl sulfate, butynediol and saccharin to bath a, the deposits morphology is markedly different. The large gold particles disappear and the surface of deposit e is smoother, more compact, and finer grained. Accordingly, the presence of additives promotes the more negative shift in the gold deposition potential on cathodic polarization of curve (e). The above phenomenon is due to the strongest absorption of three additives on the cathode, thus exhibiting the strongest effect on the morphology of gold deposits.

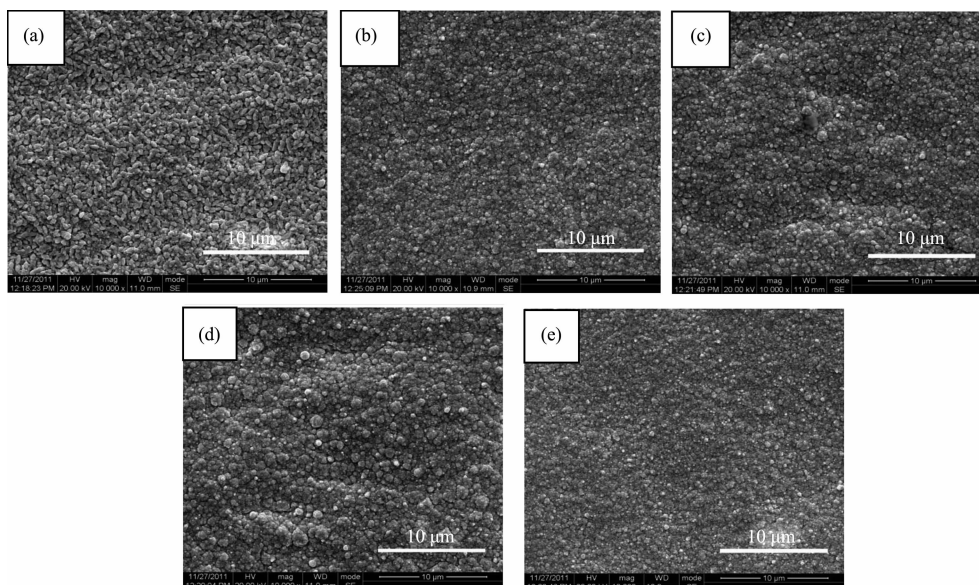


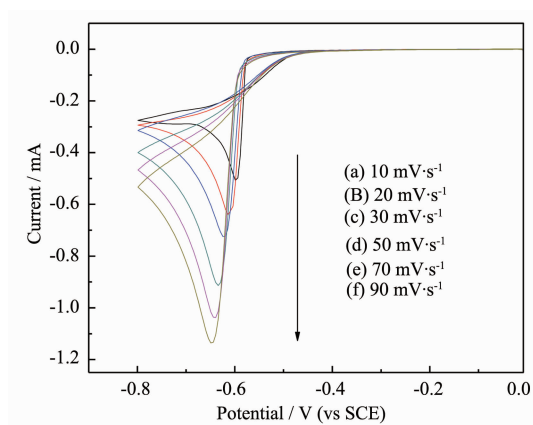
Fig.4 shows SEM images of gold deposits plated at $1.5 \text{ A} \cdot \text{dm}^{-2}$ for 10 min on copper sheets from bath without(a) or with brightening additive (b~e), respectively

2.3 Electrochemical behavior of $[\text{Au}(\text{DMH})_4]^-$ in gold plating bath

Cyclic voltammograms data for the bath with brightening

additives at various scan rates on a GCE at 45°C are shown in Fig.5.

From Fig.5, a single cathodic reduction wave is observed



(a) 10 $\text{mV} \cdot \text{s}^{-1}$; (b) 20 $\text{mV} \cdot \text{s}^{-1}$; (c) 30 $\text{mV} \cdot \text{s}^{-1}$; (d) 50 $\text{mV} \cdot \text{s}^{-1}$; (e) 70 $\text{mV} \cdot \text{s}^{-1}$; (f) 90 $\text{mV} \cdot \text{s}^{-1}$

Fig.5 Cyclic voltammograms of $[\text{Au(III)(DMH)}_4]^+$ in gold plating bath with brightening additives at various scan rates on a GCE at 45 °C

near -0.6 V on the negative scan from 0 to -0.8 V . Therefore, the cathodic wave corresponds to the reduction of Au(III) to Au . As shown in Fig.5, the cathodic peak current increases and the cathodic peak potential shifts negatively with increasing the scan rate v , indicating that reduction of Au(III) on GCE is an irreversible process^[15].

Linear sweep voltammetry was performed to study the effect of agitation on the deposition behavior of gold. The polarization data for gold deposition from the DMH-gold bath with brightening additives at a RDE at different rotation speeds are illustrated in Fig.6. Comparing the polarization curves at different rotation speeds, it can be seen that agitation is very important for gold deposition. At 0 $\text{rad} \cdot \text{s}^{-1}$ (no agitation), the limiting current density is low ($\sim 0.125 \text{ A} \cdot \text{dm}^{-2}$) and is reached almost immediately after gold started to deposit. The limiting current density increases with increasing agitation. A plot of

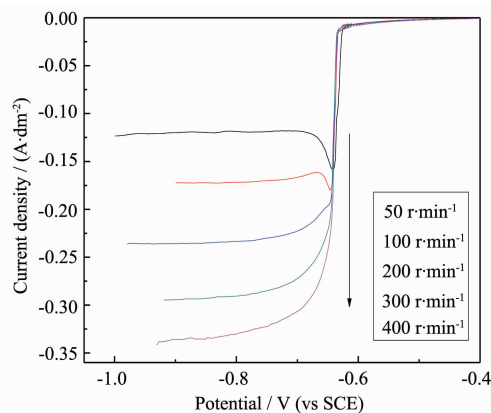


Fig.6 Polarization curves of gold deposition from the bath with brightening additives at a RDE at different rotation speeds

limiting current density, J_d obtained from linear sweep voltammetry as a function of $\omega^{1/2}$ (ω is the rotation speed, $\text{rad} \cdot \text{s}^{-1}$) for the reduction of Au(III) on a RDE is shown in Fig.7. According to Levich equation, when the electrode reaction is controlled by diffusion processes, the relationship between the limiting current I_d and rotation speed (ω) can be expressed as Eq.(2)^[16]:

$$I_d = 0.62nFAC^*D^{2/3}\gamma^{-1/6}\omega^{1/2} \quad (2)$$

where n is the number of exchanged electrons, F is the Faraday constant, A is the electrode area in cm^2 (0.07 cm^2), C^* is the gold concentration in $\text{mol} \cdot \text{cm}^{-3}$, D is the diffusion coefficient in $\text{cm}^2 \cdot \text{s}^{-1}$, γ is the dynamic viscosity in $\text{Pa} \cdot \text{s}$ and ω is the rotation speed in $\text{rad} \cdot \text{s}^{-1}$. As shown in Eq.(2), there is a linear relationship between I_d and $\omega^{1/2}$. Moreover, Fig.7 shows that the plots of the variation of limiting current density, J_d obtained from linear sweep voltammetry against $\omega^{1/2}$ are linear. It can be inferred that the electrodeposition of gold is controlled by the diffusion process. So, it can be concluded that the reduction of Au(III) to Au on a GCE is an irreversible and diffusion-controlled process.

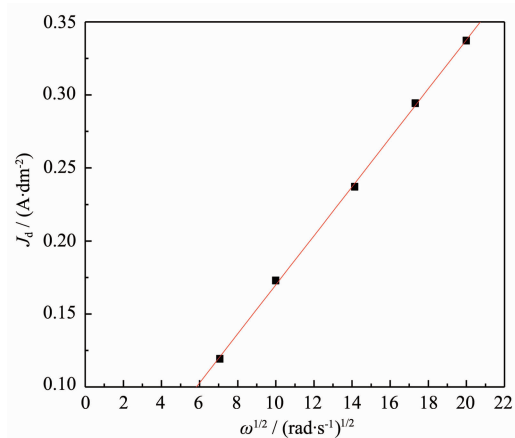


Fig.7 Limiting current density, J_d vs. $\omega^{1/2}$ for the reduction of Au(III) in gold plating bath

2.4 Properties of gold electrodeposits

The XRD pattern of the gold electrodeposits is shown in Fig.8. The gold electrodeposits include five obvious diffraction peaks of Au (111), (200), (220), (311) and (222) associated with face-centered cubic (fcc) structure, indicating that the face-centered cubic structure of gold is preserved in the gold electrodeposits. The diffraction peak intensity corresponding to the (111) plane is larger than the other peaks, indicating that the electrodeposits have well preferred orientation along

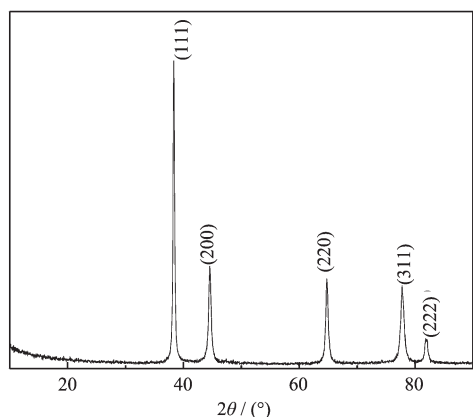


Fig.8 XRD pattern of gold electrodeposits obtained from the bath with brightening additives at $1.5 \text{ A} \cdot \text{dm}^{-2}$ for 10 min on a copper substrate

(111) direction. This is because the (111) surface is the most densely packed and hence the energetically most favorable for the surface growth for the fcc gold, as reported in the literature^[17].

To confirm the chemical state of the gold in the electrodeposits, an XPS experiment was carried out on the surface of electrodeposits as shown in Fig.9. The high-resolution Au 4f peaks show a spin-orbit doublet with two attributions at binding energy of 85.0 eV and 88.4 eV, which can be attributed to Au^0 state indicating that the gold electrodeposits are composed of pure Au^0 state.

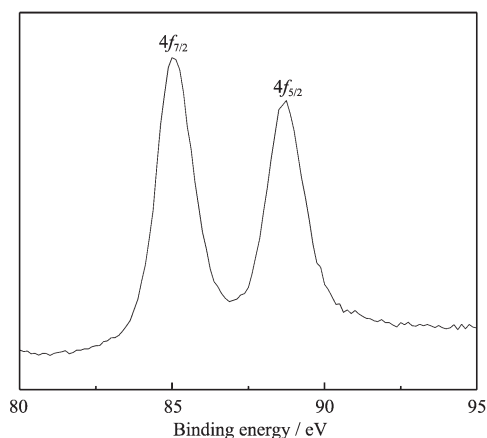
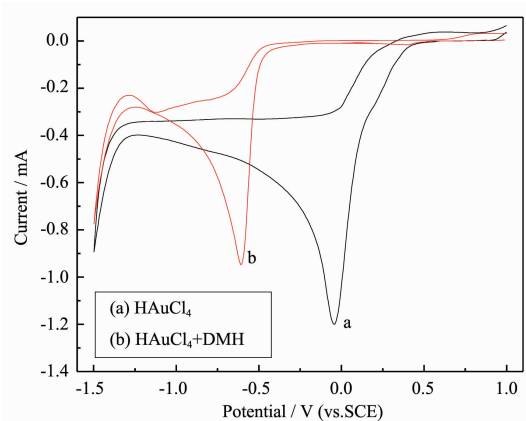


Fig.9 XPS spectra of gold electrodeposits obtained from the bath with brightening additives at $1.5 \text{ A} \cdot \text{dm}^{-2}$ for 10 min on a copper substrate

2.5 Studies on bath stability

Cyclic voltammogram for gold deposition at a GCE from a solution prepared by dissolving HAuCl_4

($0.05 \text{ mol} \cdot \text{L}^{-1}$) in a potassium phosphate buffer (pH 9~10) was shown in Fig.10a. In order to study the voltammogram of gold deposition from $[\text{Au}(\text{DMH})_4]^-$, DMH ($0.625 \text{ mol} \cdot \text{L}^{-1}$) was added to the solution of HAuCl_4 ($0.05 \text{ mol} \cdot \text{L}^{-1}$), as shown in Fig.10b. The potential was first scanned from 1.0 to -1.5 V and then back to 1.0 V at a rate of $100 \text{ mV} \cdot \text{s}^{-1}$. The voltammograms exhibit that a single cathodic wave corresponds to the reduction of $\text{Au}(\text{III})$ to Au and an area of hydrogen evolution is beyond -1.3 V . A noteworthy feature of the two curves is that the aurate ion in the absence of the ligand is reduced at more positive potentials, suggesting that the DMH^- does not undergo ligand exchange, at least during the course of the voltammetric experiment, and so $[\text{Au}(\text{DMH})_4]^-$ is very stable in bath.



(a) HAuCl_4 ($0.05 \text{ mol} \cdot \text{L}^{-1}$) in a potassium phosphate buffer; (b) HAuCl_4 ($0.05 \text{ mol} \cdot \text{L}^{-1}$) and DMH ($0.625 \text{ mol} \cdot \text{L}^{-1}$) in a potassium phosphate buffer on a GCE at a scan rate of $100 \text{ mV} \cdot \text{s}^{-1}$ at $45 ^{\circ}\text{C}$

Fig.10 Cyclic voltammograms for gold electrodeposition in two baths

In order to study the stability of the gold plating bath, fresh bath and bath standing over 6 months were investigated. The loss of bath stability is confirmed by a color change and decomposition of the solution. The fresh bath is transparent with a faint yellowish color, while the bath standing over 6 months is no discernible change in the color and no decomposition phenomenon of the bath can be observed. So there are no significant visible changes occurred in the bath standing over 6 months compared to the fresh bath.

3 Conclusions

The thick, compact and smooth pure gold electro-deposits were plated from a non-cyanide bath using DMH as complexing agent. The optimum bath with good stability is composed of $0.05 \text{ mol} \cdot \text{L}^{-1}$ HAuCl_4 , $0.625 \text{ mol} \cdot \text{L}^{-1}$ DMH, $0.4 \text{ mol} \cdot \text{L}^{-1}$ K_3PO_4 , calculated KH_2PO_4 , $0.55 \text{ mmol} \cdot \text{L}^{-1}$ of saccharin, $1.2 \text{ mmol} \cdot \text{L}^{-1}$ of butynediol and $0.17 \text{ mmol} \cdot \text{L}^{-1}$ of sodium dodecyl sulfate. Brightening additives increase the cathodic polarization and refine the grains of deposits. The results of cyclic voltammograms and linear sweep voltametrys show that the reduction of Au (III) to Au on a GCE is an irreversible process and controlled by the diffusion of Au (III). XRD pattern indicates that the gold deposits have a preferential orientation along (111) direction.

Acknowledgements: The authors would like to thank the Research Center of Laser Fusion under China Academy of Engineering Physics in Mianyang for the financial support.

References:

- [1] Haferkamp H, Niemeyer M, Boehm R, et al. *Mater. Sci. Forum*, **2000**,**350**:31-35.
- [2] Gemmler A, Keller W, Ritcher H, et al. *Plat. Surf. Finish*, **1994**,**81**(8):52-58
- [3] Liu J, Duan J L, Toimil M E, et al. *Nanotechnology*, **2006**,**17**(8):1922-1926
- [4] Christie I R, Cameron B P, et al. *Gold Bull.*, **1994**,**27**(1):12-20
- [5] Osaka T, Kodera A, Misato T, et al. *J. Electrochem. Soc.*, **1997**,**144**(10):3462-3469
- [6] Masaru K, Kazutaka S, Yuta M, et al. *Electrochim Acta*, **2007**,**53**(1):11-15
- [7] Natter H, Hempelmann R, et al. *Electrochim Acta*, **2003**,**49**:51-61
- [8] Osaka T, Kodera A, Misato T, et al. *J. Electrochem. Soc.*, **1997**,**144**(10):3462-3469
- [9] Green T A, Liew M J, Roy S, et al. *J. Electrochem. Soc.*, **2003**,**150**(3):104-110
- [10] Honma H, Hagiwara K, et al. *J. Electrochem. Soc.*, **1995**, **142**(1):81-87
- [11] Morrissey R J, Versatile A, et al. *Plat. Surf. Finish*, **1993**,**80**(4):75-79
- [12] Honma H, Kagaya Y, et al. *J. Electrochem. Soc.*, **1993**,**140**(9):135-137
- [13] Liew M J, Sobri S, Roy S, et al. *Electrochimica Acta*, **2005**,**51**(5):877-881
- [14] Ohtani Y, Sugawara K, Nemoto K J, et al. *Surface Finish. Soc. Japan*, **2006**,**57**(2):167-171
- [15] Jayakumar M, Venkatesan K A, Srinivasan T G, et al. *Electrochimica Acta*, **2007**,**52**(24):7121-7127
- [16] LU J F(卢俊峰). *Thesis for the Doctorate of Harbin Institute of Technology University*(哈尔滨工业大学博士论文). **2007**.
- [17] Wang J G, Tian M L, Mallouk T E, et al. *J. Phys. Chem.*, **2004**,**108**:841-845